Continuous monitoring of near-bottom mesoplankton communities in the East China Sea during a series of typhoons

Mary M. Grossmann[1]*, Scott M. Gallager[2], Satoshi Mitarai[1]

[1]: Marine Biophysics Unit, Okinawa Institute of Science and Technology, 1919-1 Tancha, Onna, Okinawa, 904-0495 Japan

[2]: Department of Biology, Woods Hole Oceanographic institution, MA, USA

* Corresponding author: mary.grossmann@oist.jp

Marine Biophysics Unit, Okinawa Institute of Science and Technology, 1919-1 Tancha, Onna, Okinawa, 904-0495 Japan; Tel: (+81) 98-966-1064.

Abstract

Typhoons are a common feature of summer and autumn months in the East China Sea. These events often promote phytoplankton growth in surface waters as a result of upwelling and transport of nutrients, but their effects on sub-surface waters and ecosystems are little known. Furthermore, biological studies tend to focus on phytoplankton (using chlorophyll *a* assays), rather than on heterotrophic zooplankton. Indeed, measurements of biological and physicochemical changes induced by the storms are difficult to perform and risky, using standard shipboard sampling techniques. Using a camera mounted on an underwater, cabled observatory system in shallow coastal waters of Okinawa, Japan, we collected the first continuous, *in-situ* observations of the near-bottom, mesoplankton community during a series of typhoons. An increase in diatoms and radiolarians was found during all typhoons, whereas the response of larger zooplankton groups was variable between typhoons. A bloom of *Trichodesmium* cyanobacteria and diatoms was seen after a series of typhoons, while the total chlorophyll *a* concentration remained nearly unchanged at the sampling location. These findings shed new light on short-term responses of sub-surface ecosystems during typhoons.

Keywords: Typhoon; *OCTOPUS* cabled observatory; *Trichodesmium*; benthic resuspension; mesozooplankton.

Introduction

The East China Sea is a warm, oligotrophic, marginal sea, in which nutrients are limiting to phytoplankton growth in both the surface and sub-surface layers (Hashihama *et al*. 2013; Hung *et al.* 2013a; Wu *et al.* 2003). This region is usually swept by typhoons (tropical cyclones) in the summer and autumn months, sometimes repeatedly. These storms often cause cooling at the surface, and an increase in nutrient concentrations, which in turn stimulate post-typhoon phytoplankton blooms in surface waters (e.g. Chen *et al.* 2009; Hung and Gong, 2011; Liu *et al.* 2013; Tsuchiya *et al.* 2013; 2014; Zheng and Tang, 2007). Upwelling of deep water, as well as post-typhoon increases in surface and sub-surface primary production, are believed to be beneficial for higher trophic levels by increasing the flux of particulate organic matter toward the sediment (Hung and Gong, 2011; Hung *et al.* 2010), but the short-term response of heterotrophic communities to typhoons has yet to be studied.

Indeed, marine studies during typhoons are hindered by the storms, which render traditional shipboard sampling activities virtually impossible. For these reasons, the bio-physical effects of typhoons are primarily studied using satellite monitoring, gathering such information as sea surface height, temperature, or chlorophyll *a* concentration. However, these methods can only gather data regarding the upper layer of the water column. This may induce an underestimation of the effect of typhoons on the water column, as strong storms have been shown to induce sub-surface increases in chlorophyll *a* concentration that remain undetected by remote sensing techniques (Ye *et al.* 2013). Additionally, satellite monitoring is restricted to the measurement of detectable photosynthetic pigments, and is not adapted to the study of zooplankton communities.

As a result, the effect of typhoons on the physical oceanography and biogeochemistry of surface waters and the autotrophic communities found there is well documented (D'Asaro *et al.* 2011; Pun *et al.* 2011). But studies of the response of heterotrophic plankton groups to these storms are lacking, and the impact of typhoons on sub-surface waters is still largely unknown. This is even more important in shallow coastal ecosystems, where compositional changes in sub-surface water masses necessarily have a more direct impact on benthic ecosystems.

Installed at a depth of 20 m on the edge of a coral reef on Okinawa Island, in the central East China Sea, the *OCTOPUS* (*OIST Cabled Teleoperational Observatory Platform for Undersea Surveillance*) system provides continuous biological and physical measurements of coastal, sub-surface waters. Using an underwater plankton camera installed on the observatory, we studied the impact of typhoons of varying intensity on the near-bottom mesophyto- and zooplankton communities.

Material and Methods

OCTOPUS is comprised of an OceanCube (Woods Hole Oceanographic Institution, USA) cabled observatory system installed on the seafloor at about 20 m depth on the northwestern coast of Okinawa Island, Japan (26°42.79'N, 127°52.13'E) (Fig. 1). Data from all sensors and cameras are sent to a shore-based server in real time at full resolution on a single-mode fiber optic cable. An Acoustic Vector Current Meter (Nortek, USA) and Water Quality Monitor (WQM: WETLabs, USA) attached to the main node measured physical and optical properties of the water at 20 m depth (Table 1). The chlorophyll *a*, turbidity and coloured dissolved organic material (CDOM) sensors of the WQM were calibrated at 24.1°C at WetLabs in September 1st, 2013. No further calibrations were performed during the 3-month deployment. An Acoustic Doppler Current Profiler (RD Instruments, USA), positioned 45 m to the West of the main node, was used to measure surface wave height.

A Continuous Plankton Imaging and Classification Sensor (CPICS, Woods Hole Oceanographic Institution, USA) was installed on the main node, about 1.60 m above the seafloor, equipped with a Prosilica GT 1380 camera and a synchronized strobe light in waterproof housings, imaging an 8.00 x 7.50 x 0.55 mm volume of water 4 times per second (0.48 L/hr). Images (1380 x 1024 pixels) were processed in real-time on shore to bound all objects exceeding 645 μm^2 (100 adjacent pixels) as "Regions of Interest" (ROI), using graphic processing hardware and customized software. The software is capable of recording up to 999 ROI per full image to hard disk, a limit that was never reached during the present study. ROI were manually sorted into 11 categories representing the main plankton taxonomic groups present in the sampling area: filamentous cyanobacteria (*Trichodesmium* spp.), diatoms, radiolarians (primarily acantharians), foraminiferans, copepods, isopods, cnidarians, other zooplankton (e.g. appendicularians, ostracods, and larval molluscs), mysids, and fish; and a marine snow 'particle' category regrouping all non-living particles (Fig. 2). The size range of particles was 100 µm to 10 mm in length.

Plankton images were collected between August 28th and November 9th, 2013. Typhoons were identified based on data provided by the Regional Specialized Meteorological Center (Japan Meteorological Agency, 2014). All dates and times are listed in universal time (UTC), local time being UTC+09:00. Night lasted about 12 hr during the studied period, from 9:00 to 21:00 UTC. All data were analyzed in 1-hr bins. Using the R package "*vegan*" (Oksanen *et al.* 2013), analyses of similarity (ANOSIM) were performed on binned plankton abundance data to test the effect of wave height on plankton distribution.

Results

1. Baseline community

The *OCTOPUS* cabled observatory is installed on the northwestern shore of Okinawa Island, Japan, on the northeastern edge of the channel separating Motobu Point from Ie Island (Fig. 1). The closest river to the sampling site is located about 6 km south of the sampling point, just north of Sesoko Island. The mean depth of the station during the sampling period was 19.34 m, with an average 1.2 m tidal variation (Fig. 3). The mean temperature above the seafloor was 29.2° C in August, decreasing to 25.7° C in early November. Salinity, dissolved oxygen, chlorophyll *a*, CDOM and turbidity were not measured until September 9th. Low salinities and relatively high dissolved oxygen concentrations were observed throughout the sampling period, with average values of 34.60 and 4.52 mL/L, respectively (Fig.3). Chlorophyll *a*, CDOM, and turbidity were low except during typhoons, with average values of 0.22 µg/L, 0.21 ppb QSDE and 0.08 NTU, respectively.

Near-continuous imaging at the cabled observatory between August 28th and November 9th, 2013, yielded images of 50,320 planktonic organisms, and about 340,000 marine snow particles ranging between 100 µm and 10 mm in length. On average, the particle abundance at the observation point was 400 particles/hr, increasing to 2,000/hr when wave heights exceeded 2.0 m. Zooplankton was the dominant plankton group, with copepods (primarily Calanoida) and radiolarians, representing 36.27 and 25.24% of total plankton, respectively (Table 2). These groups were also the most common temporally, having been observed in 97% of all sampling hours. Because they were imaged almost exclusively during periods of high turbidity and wave height (Fig. 4, 5), Foraminifera were assumed to be of benthic origin, their presence in the CPICS data representative of benthic resuspension events. Phytoplankton, representing ~11% of total plankton, were predominantly diatoms (primarily pinnates) and nitrogen-fixing cyanobacteria of the genus *Trichodesmium*. *Trichodesmium*, diatoms and radiolarians were equally abundant throughout the day. Copepods, cnidarians, and 'other zooplankton' also did not show diel patterns of abundance at the studied taxonomic levels, but peaks of abundance were sometimes seen at night, occurring as single-species swarms. Juvenile isopods and mysids did not have a high mean abundance, but rather occurred in periodic, large swarms, at night, at which times they reached concentrations of over 250 ind./hr. Fish (mainly of the family Gobiidae) were found almost exclusively during the day (Table 2). A temperature-salinity-plankton plot (Gallager *et al.* 1996) showed mysids, fish, isopods and jellyfish were not present during times with highest waves (Fig. 4), while on the contrary, foraminiferans were primarily found when wave height exceeded 2 m.

2. September typhoons

Measurement of significant wave height showed a succession of relatively calm periods with waves less than 1 m, and the passing of several typhoons of varying intensity (Fig. 3). The first typhoon (T1317) occurred on September 3rd and 4th, with waves up to 4.0 m. A spiked decrease in temperature of 1.5°C was recorded right after maximal wave heights. Strong wind was recorded on September 16th and 17th (Japan Meteorological Agency, 2014), but wave height did not exceed 2.3 m, and only small changes were observed in other physicochemical parameters.

Numbers of marine snow particles were strongly correlated with wave height (ANOVA, $p<0.001$), with a maximum of 7,500 marine snow particles observed on September 3rd between 6 and 7 pm UTC (Fig. 5) during Typhoon T1317. Mysids showed the greatest increase in abundance during the typhoon, with a maximum of 138 ind/hr, and *Trichodesmium*, diatom, and radiolarian abundances were also positively correlated with wave height (ANOVA, $p<0.001$). Other plankton categories did not show significant variations in abundance during typhoon T1317. Foraminiferan abundance increased only slightly during the September typhoon, with fewer than 3 individuals/hr.

<u>3. October typhoons</u>

On October 3rd, waves up to 3.2 m were recorded, followed by three large typhoons of increasing intensity, on October 7th (T1324: waves up to 3.9 m), 15 and 16th (T1326: waves up to 4.9 m) and from October 24 to 26th (T1327: waves greater than 5 m for 24 hr, with a maximum of 6.1 m). During T1326, temperature and salinity decreased concurrently during 2 events, each lasting about 3 hr (Fig. 6a). On the contrary, during T1327, salinity decreased by 0.5, followed by a temperature decrease of nearly 2.5°C that was associated with relatively higher salinity values (Fig. 6b). During both typhoons, each low salinity or low temperature event was associated with an increase in particle numbers. The last two typhoons were also accompanied by an increase in turbidity, chlorophyll *a*, and CDOM concentrations. During T1324 on October 7th, a spiked decrease in temperature, associated with an increase in salinity was observed before wave height increased. The highest wave heights were associated with a distinct decrease in salinity and high turbidity levels, but no significant variation in temperature, CDOM or Chl *a* was measured.

The October typhoons were accompanied by a significant increase in marine snow particles (ANOVA, $p<0.001$). However, the highest concentrations of marine snow were recorded on September 3rd (Fig. 5) when wave heights did not exceed 4.0 m, while the two largest typhoons in October showed smaller increases in particle numbers (no imaging was performed during the October 7th typhoon due to a power failure), with maxima of 3,700 and 4,200 marine snow particles/hr during typhoons T1326 and T1327, respectively (Fig. 6). Wave height also showed a positive correlation with the abundance of marine snow particles relative to plankton, with marine snow representing 97.4% of the hourly particles on average when wave height exceeded 4.0 m, against an average of 90% during times with smaller waves. During T1326, increased wave height caused a significant increase in abundance of diatoms, foraminiferans, radiolarians, copepods, and other zooplankton, and a significant decrease in the abundance of fish (ANOVA, $p<0.001$). The abundance of *Trichodesmium*, isopods, medusa, and mysids did not show a significant variation in relation with waver height. In contrast, during T1327, the abundance of copepods was not correlated with wave height, while isopods showed a significant negative correlation with wave height (ANOVA, $p<0.001$). Analyses of similarity (ANOSIM: wave height ~ time of day, $\alpha = 0.05$) showed that wave height had no significant influence on diel patterns of abundance of the plankton groups.

4. Post-typhoon

By mid-day on October 28th, turbidity, CDOM, and wave-height had returned to pre-typhoon values and wave height did not exceed 1.0 m except for a couple of hours on November 4th. Chlorophyll *a* concentrations remained constant, around 0.25 µg/L until November 9th.

From October 29th to November 4th, a significant increase in abundance was found for all plankton categories except foraminiferans and isopods (ANOVA, $p<0.001$), independently from an increase in wave height.

Discussion

In August and September, warm, oligotrophic water was found in the near-bottom layer at the sampling location, with low chlorophyll *a* and CDOM concentrations, as well as low turbidity, but with relatively high oxygen concentrations (Fig. 3). Salinity remained low (<35.0) throughout the sampling period, but a gradual decrease in temperature was observed.

Since the CPICS camera recorded only organisms with profiles larger than 645 μm^2, the phytoplankton community appeared to be composed entirely of diatoms, large *Trichodesmium* chains, and aggregates. However, the phytoplankton community observed about 10 km south of the sampling area in 1998 and 1999 was dominated by pico- and nano-phytoplankton, representing 52-55% and 28-34% of the total chlorophyll *a* concentration, respectively, with larger plankton groups, such as diatoms representing only 11 - 17% (Tada *et al.* 1999; 2003). These results match those from temperate regions having low chlorophyll *a* concentrations (e.g. Iriate and Purdie, 1994). The latter studies showed only a limited effect of variations in abundance of micro-phytoplankon on total chlorophyll *a* concentration measured in picoplankton-dominated systems (Iriate and Purdie, 1994; Tada *et al.* 1999; 2003). Therefore, we suspect that *in-situ* chlorophyll *a* measurements performed at the observatory may not reflect larger organisms, such as *Trichodesmium* and diatoms, but rather the abundance of pico- and nano-phytoplankton that are too small to be recorded by the CPICS camera or, in times of high waves, of resuspended micro-phytobenthos (Koh *et al*. 2006;

Suga and Montani 2012). These smaller plankton groups were beyond the scope of the present study, but will form the basis of further studies of the plankton dynamics in this area.

The zooplankton community was dominated by copepods, primarily small calanoids, which did not show any significant diel patterns of abundance at this taxonomic level. Few copepods were imaged attached to marine snow particles, suggesting a predominantly herbivorous or carnivorous community. Radiolarians were the next most abundant group, both numerically and temporally (Table 2). These organisms often contain endosymbiotic, photosynthetic algae (Adl *et al.* 2012), allowing them to obtain energy photosynthetically in times of low prey availability. The dominant predatory groups were juvenile isopods and mysids, which were nocturnal, and young gobiid fish, that were strictly diurnal. Gelatinous carnivores were rare, the predominant forms being young anthomedusan jellyfish, newly released from polyps colonizing the CPICS camera and surrounding equipment. While polyp stages were observed actively feeding (not shown), no stomach contents could be observed in the small medusae.

Three typhoons were monitored at the cabled observatory between September and November 2013. The typhoons caused an increase in wave height, directly followed by an increase in the number of marine snow particles recorded by the CPICS camera. The typhoon of September (Fig. 3) was characterized by moderate maximum wave heights and a moderate increase in foraminiferan abundance (Fig. 5), reflective of limited sediment resuspension. Although water turbidity was not measured at this time, a large-area *in-situ* camera confirmed much higher visibility throughout the September typhoon compared to the October typhoons. However, water temperature decreased by up to 1.5°C, and this typhoon corresponded to the largest and fastest increase in both marine snow and non-swimming plankton (*Trichodesmium*, diatoms, radiolarians) concentrations (Fig. 5). Large swarms of mysids and some larger zooplankton were also observed, possibly taking advantage of increased concentrations of diatoms and particles.

In contrast to September 3rd, the two typhoons in October, for which CPICS data are available (T1326 and T1327), had much higher physicochemical and biological impacts, with spiked decreases in salinity following the increase in wave height (Fig. 6), suggesting possible mixing with surface waters. A distinct decrease in temperature was also observed, corresponding to high particle numbers. The October typhoons also caused an increase in CDOM, chlorophyll *a*, and turbidity (Fig. 3), indicating a possible re-suspension of sediment. This hypothesis was corroborated by the high abundance of foraminiferans (Fig. 5) and macroalgae shreds observed during the typhoons, as well as the presence of two small post-larval starfish, imaged during the typhoon, about 1.5 m off the bottom (Fig. 2i). The October typhoons caused an increase in abundance of non-swimming plankton such as radiolarians and diatoms, and of the ‘other zooplankton’ category, primarily in the form of eggs and small molluscs. Fish were almost completely absent during times of maximum wave heights, possibly due to increased turbidity at the sampling location. The increase in chlorophyll *a* observed during the October typhoons was most likely the result of high turbidity and resuspension of micro-phytobenthos brought on by the typhoons, rather than a sudden increase in nano- and pico-phytoplankton concentrations (Suga and Montani 2012). Re-suspended benthic particulate organic matter (POM) is thought to represent as much as 93% of the POM flux in the western part of the East China Sea (Hung *et al*. 2013a), thereby contributing greatly to surface productivity along the continental shelf. Along the Okinawa coast, the flux of resuspended benthic POM created by autumnal typhoons would benefit both the plankton and the coral reef community surrounding the observatory site. However, high particle abundances, of benthic origin, were restricted to the duration of the typhoon in the present study (Fig. 6), and did not continue after the typhoon, as was reported by Hung and Gong (2011) from surface waters in the East China Sea.

Different plankton responses observed between the September and October typhoons might be explained by the positioning of the typhoon in relation to Okinawa Island and the sampling site (Fig. 1). In October, all three typhoons originated from the southeast, and the observatory site was therefore somewhat sheltered from the winds by Okinawa Island. In September, however, the typhoon followed a north to northeast path just west of the island. The large increase in particles and non-swimming plankton, such as radiolarians, during this typhoon, may reflect increased current speeds as the typhoon pushed water through the channel between Motobu Point and Ie Island (Fig 1). Further studies, including the measurement of current speeds and direction would be necessary to completely explain the different biological responses observed.

On October 29th, three days after the last typhoon, a short-lived (6-day) bloom of diatoms and *Trichodesmium* (Fig. 5) was observed, possibly promoted by precipitation, vertical mixing, and benthic re-suspension during the October typhoons. This bloom was accompanied by an increase in abundance of other zooplankton categories, possibly due to increased food supply. Contrary to previous reports from surface waters in the southern East China Sea (Hung and Gong 2011), no significant increase in the proportion of centric diatoms was noted after the typhoons. Benthic re-suspension caused by the typhoons may have provided nitrates and other important nutrients, such as iron or phosphorous to the water column, similar to what was reported from the southern East China Sea (Hung *et al*. 2013b; Shih *et al*. 2013). This hypothesis is supported by the increase in *Trichodesmium*, as well as diatoms. These nitrogen-fixing cyanobacteria are not nitrate-dependent, but an iron scarcity has been suggested as limiting their abundance in the South China Sea (Wu *et* *al.* 2003). Additionally, labile phosphate represents less than 30% of the dissolved organic phosphate (DOP) concentration in the East China Sea (Hashihama *et al.* 2013), indicating a possible phosphate limitation of phytoplankton in the coastal waters of Okinawa (Guo *et al.* 2012). The post-typhoon increase in abundance of *Trichodesmium* is contrary to what was observed after the passage of a hurricane in the North Atlantic (Davis and McGillicully, 2006), indicating that the response of these organisms may vary depending on the physical oceanographic and biological conditions of the sampling location. Chlorophyll *a* concentrations, most certainly reflecting pico- and nano-phytoplankton communities that were too small to be imaged by the CPICS camera (see above), did not show a significant increase at the end of October, confirming that typhoons may not benefit all autotrophic plankton groups equally (Chen *et al*. 2009; Chung *et al*. 2012). Indeed, in similar oligotrophic, pico-phytoplankton-dominated communities, increased nutrient concentrations due to upwelling events have been shown to trigger diatom blooms preferentially (Chung *et al*. 2012; Maita and Odate 1988). In a study of the relative abundances of the different phytoplankton size classes found south of the observatory site in 1998 and 1999, several peaks in abundance of the larger micro-phytoplankton class (> 20 µm) relative to smaller phytoplankton groups were observed during the autumn months (Tada *et al*. 2003), which might indicate post-typhoon diatom blooms. Similar to our results, the increase in meso-phytoplankton biomass was not reflected in the total chlorophyll *a* concentration.

Conclusions

This study presents the first observations of near-bottom mesoplankton communities above a coral reef and their responses to typhoons of varying intensity. The first typhoon, in early September, caused a large increase in abundance of nearly all studied plankton categories. In contrast, plankton communities reacted differently to the larger October typhoons, with less mobile organisms increasing in abundance during the typhoons, while larger zooplankton disappeared from the sampling area. The constant monitoring of physicochemical parameters during the October typhoons showed that increased wave height caused a spiked decrease in salinity, as well as a slower, more prolonged decrease in temperature, corresponding to higher particle concentrations. At the end of the typhoon season, a bloom of diatoms and *Trichodesmium* cyanobacteria appeared in the sampling area, but the total chlorophyll *a* concentration did not increase significantly. Further studies incorporating different sampling techniques will be necessary to simultaneously examine the whole size range of the phyto- and zooplankton communities, as well as nutrients such as phosphorus or iron in this coral reef ecosystem, in order to better understand the interactions among these organisms and changes resulting from major environmental events such as tropical cyclones.

Acknowledgements

We are grateful to the editor and two anonymous reviewers for critical and constructive comments on the manuscript. We also thank the captain and crew of the *Kuroshio-maru*, Amber York and the rest of the WHOI Ocean Cube engineering team, Shohei Nakada and Yukiko Murayabashi, Koichi Toda, Takeshi Sannomiya, Yuko Hasegawa and the rest of the Marine Science Resources Section, OIST, for the installation and maintenance of the *OCTOPUS* observatory. We also thank Steven D. Aird, for English editing of the manuscript. MMG also thanks Dr. Dhugal Lindsay, Naoto Jimi, Michitaka Shimomura and Dr. Russell Hopcroft for help with taxonomic identification of the CPICS ROIs. This work was funded by the Special Framework budget, Okinawa Promotion for Education and Research Project awarded to OIST for the 2012 fiscal year.

References

Adl SM, Simpson AG, Lane CE, Lukeš J, Bass D, Bowser SS, Brown MW, Burki F, Dunthorn M, Hampl V, Heiss A, Hoppenrath M, Lara E, le Gall L, Lynn DH, McManus H, Mitchell EAD, Mozley-Stanridge SE, Parfrey LW, Pawlowski J, Rueckert S, Shadwick L, Schoch CL, Smirnov A, Spiegel FW (2012) The revised classification of eucaryotes. J Eucaryot Microbiol 59(5): 429–493

Chen YL, Chen H-Y, Jan S, Tuo S (2009) Phytoplankton productivity enhancement and assemblage change in the upstream Kuroshio after typhoons. Mar Ecol Prog Ser 385: 111–126

Chung C-C, Gong G-C, Hung C-C (2012) Effect of Typhoon Morakot on microphytoplankton population dynamics in the subtropical Northwest Pacific. Mar Ecol Prog Ser 448: 39–49

D’Asaro EP, Black L, Harr S, Jayne S, Lin I-I, Lee C, Morzel J, Mrvaljevic R, Niiler PP, Rainville L, Sanford T, Yang TY (2011) Typhoon-ocean interaction in the western North Pacific: Part 1. Oceanography 24(4): 24–31

Davis CS, McGillicully Jr. DJ (2006) Transatlantic abundance of the N_2-fixing colonial cyanobacterium Trichodesmium. Science 312. doi: 10.1126/science.1123570

Gallager SM, Davis CS, Epstein AW, Solow A, Beardsley RC (1996) High-resolution observations of plankton spatial distributions correlated with hydrography in the Great South Channel, Georges Bank. Deep-Sea Res II 43(7-8): 1627–1663

Guo X, Zhu X-H, Wu Q-S, Huang D (2012) The Kuroshio nutrient stream and its temporal variation in the East China Sea. J Geophys Res 177. doi:10.1029/2011JC007292

Hung C-C, Gong G-C, Chou C-C, Lee M-A, Chang Y, Chen H-Y, Huang S-J, Yang Y, Yang W-R, Chung W-C, Li S-L, Laws E (2010) The effect of typhoon on particulate organic carbon flux in the southern East China Sea. Biogeosciences 7: 3007–3018

Hung C-C, Gong G-C (2011) Biochemical responses in the southern East China Sea after typhoons. Oceanography 24(4): 42–51

Hung C-C, Tseng C-W, Gong G-C, Chen K-S, Chen M-H, Hsu S-C (2013a) Fluxes of particulate organic carbon in the East China Sea in summer. Biogeosciences 10: 6469–6484

Hung C-C, Chung C-C, Gong G-C, Jan S, Tsai Y, Chen K-S, Chou WC, Lee M-A, Chang Y, Chen M-H, Yang W-R, Tseng C-J, Gawarkiewicz G (2013b) Nutrient supply in the Southern East China Sea after Typhoon Morakot. J Mar Res 71: 133–150

Iriate A, Purdie DA (1994) Size distribution of chlorophyll a biomass and primary production in a temperate estuary (Southampton Water): the contribution of photosynthetic picoplankton. Mar Ecol Prog Ser 115: 283–297

Japan Meteorological Agency, Regional Specialized Meteorological Center, Tropical Cyclone Information (2014) http://www.jma.go.jp/en/typh/index.html Accessed on 22 April, 2014

Koh C-H, Khim JS, Araki H, Yamanishi H, Mogi H, Koga K (2006) Tidal resuspension of microphytobenthic chlorophyll *a* in a Nanaura mudflat, Saga, Ariake Sea, Japan: flood–ebb and spring–neap variations. Mar Ecol Prog Ser 312: 85–100

Liu H, Hu Z, Huang L, Huang H, Chen Z, Song X, Ke Z, Zhou L (2013) Biological response to typhoon in northern South China Sea: a case study of “Koppu”. Cont. Shelf Res. 68: 123–132

Maita Y, Odate T (1988) Seasonal changes in size-fractionated primary production and nutrient concentrations in the temperate neretic water of Funka Bay, Japan. J Oceanogr Soc Japan 44: 268–279

Oksanen J, Blanchet FG, Kindt R, Legendre P, Minchin PR, O’Hara RB, Simpson GL, Solymos P, Steven MH, Wagner H (2013) Community ecology package: http://cran.r-project.org, http://vegan.r-forge.r-project.org/ Accessed on 22 April, 2014

Pun IF, Chang Y-T, Lin II, Tang TY, Lien R-C (2011) Typhoon-ocean interaction in the western North Pacific: Part 2. Oceanography 24(4): 32–41

Shih Y-Y, Hsieh J-S, Gong G-C, Hung C-C, Chou W-C, Lee M-A, Chen M-H, Wu C-R (2013) Field observations of changes in SST, chlorophyll and POC flux in the southern East China Sea before and after the passage of Typhoon Jangmi. Terr Atmos Sci 24(5): 899–910

Suga N, Montani S (2012) The effect of microphytobenthic resuspension on suspended particulate matter dynamics in a shallow lagoon in Hokkaido, Japan. In: Kawaguchi M, Misaki K, Sato H, Yokokawa T, Itai T, Nguyen TM, Ono J, Tanabe S (Eds.) Interdisciplinary studies on environmental chemistry – environmental pollution and ecotoxycology. Terrapub, Japan. pp. 353–365

Tada K, Yamada M, Takemura A, Nakano Y (1999) Size distribution of phytoplankton community in oligotrophic tropical coastal waters. La Mer 36: 139–145.

Tada K, Sakai K, Nakano Y, Takemura A, Montani S (2003) Size-fractionated phytoplankton biomass in coral reef waters off Sesoko Island, Okinawa, Japan. J Plankton Res 25:8 991–997

Tsuchiya K, Yoshiki T, Nakajima R, Miyaguchi H, Kuwahara VS, Taguchi S, Kikuchi T, Toda T (2013) Typhoon-driven variations in primary production and phytoplankton assemblages in Sagami Bay, Japan: a case study of typhoon Mawar (T0511). Plankton Benthos Res 8(2): 74–87

Tsuchiya K, Kuwahara VS, Yoshiki T, Nakajima R, Miyaguchi H, Kumekawa N, Kikuchi T, Toda T (2014) Phytoplankton community response and succession in relation to typhoon passages in the coastal waters of Japan. J Plankton Res 36(2): 424–438

Wu J, Chung S-W, Wen L-S, Liu K-K, Chen YL, Chen H-Y, Karl DM (2003) Dissolved inorganic phosphorus, dissolved iron, and Trichodesmium in the oligotrophic South China Sea. Global Biochem Cy 17(1): 1–10.

Ye HJ, Sui Y, Tang DL, Afanasyev YD (2013) A subsurface chlorophyll a bloom induced by typhoon in the South China Sea. J Mar Syst 128: 138–145

Zheng GM, Tang DL (2007) Offshore and nearshore chlorophyll increases induced by typhoon winds and subsequent terrestrial rainwater runoff. Mar Ecol Prog Ser 333: 61–74

Table Legends

Table 1. Characteristics and sampling period of measured physicochemical, environmental parameters.

Table 2. Median and maximum abundance (counts/hr), relative nighttime abundance (100 * nighttime category abundance / total category abundance), total relative abundance (100 * total category abundance / total plankton abundance), and temporal presence (100 * number of hours present / total number of hours sampled) of particle and plankton types over the sampling period

Figure Legends

Figure 1. Map of the sampling area showing the position of the *OCTOPUS* observatory (star), and tracks of the epicenters of the four typhoons studied (data obtained from the Japan Meteorological Agency, 2014). Track width indicates relative wind strength of the typhoons. Dates are given in UTC.

Figure 2. Examples of the 11 CPICS image categories: **a.** marine snow; **b.** *Trichodesmium* spp.; **c.** diatoms; **d.** radiolarians; **e.** foraminiferans; **f.** copepods; **g.** isopods; **h.** cnidarians; **i.-j.** 'other zooplankton' (**i.** adult starfish; **j.** chaetognath); **k.** mysids; **l.** fish. Scale bar = 500 µm except for j, k, l: 1,000 µm.

Figure 3. Temporal variation of depth (m), temperature (°C), salinity, dissolved oxygen (DO; mL/L), turbidity (NTU), CDOM (ppb QSDE), chlorophyll *a* (µg/L), and significant wave height (m) measured in the near-bottom layer at the observation site between August 28th and November 9th, 2013. Colour scale represents significant wave height (m), gray shading indicates missing wave height information. Boxes correspond to typhoons.

Figure 4. Distribution of marine snow and plankton categories depending on temperature and salinity during the sampling period. Colour scale represents significant wave height (m), gray shading indicates missing wave height information.

Figure 5. Temporal variation in abundance (counts/hr) of particle and plankton types during the sampling period. Colour scale represents significant wave height (m), gray shading indicates missing wave height information. White boxes correspond to typhoons.

Figure 6. Salinity, water temperature (°C), significant wave height (m), and marine snow particle concentrations (particles/hr), during a. Typhoon T1326, b. Typhoon T1327.

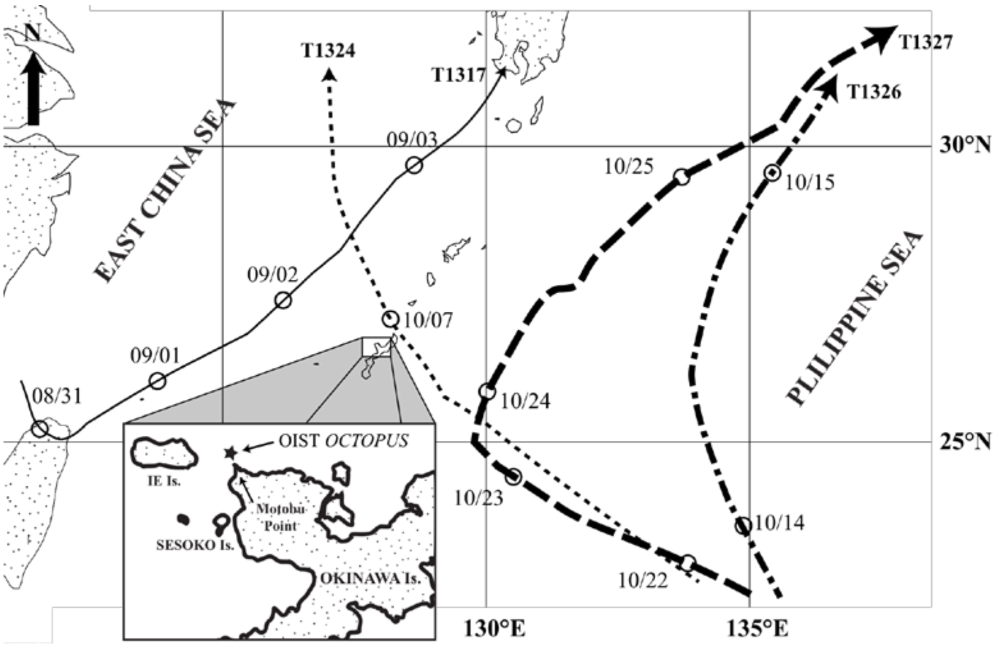

Figure 1. Map of the sampling area showing the position of the *OCTOPUS* observatory (star), and tracks of the epicenters of the four typhoons studied (data obtained from the Japan Meteorological Agency, 2014). Track width indicates relative wind strength of the typhoons. Dates are given in UTC.

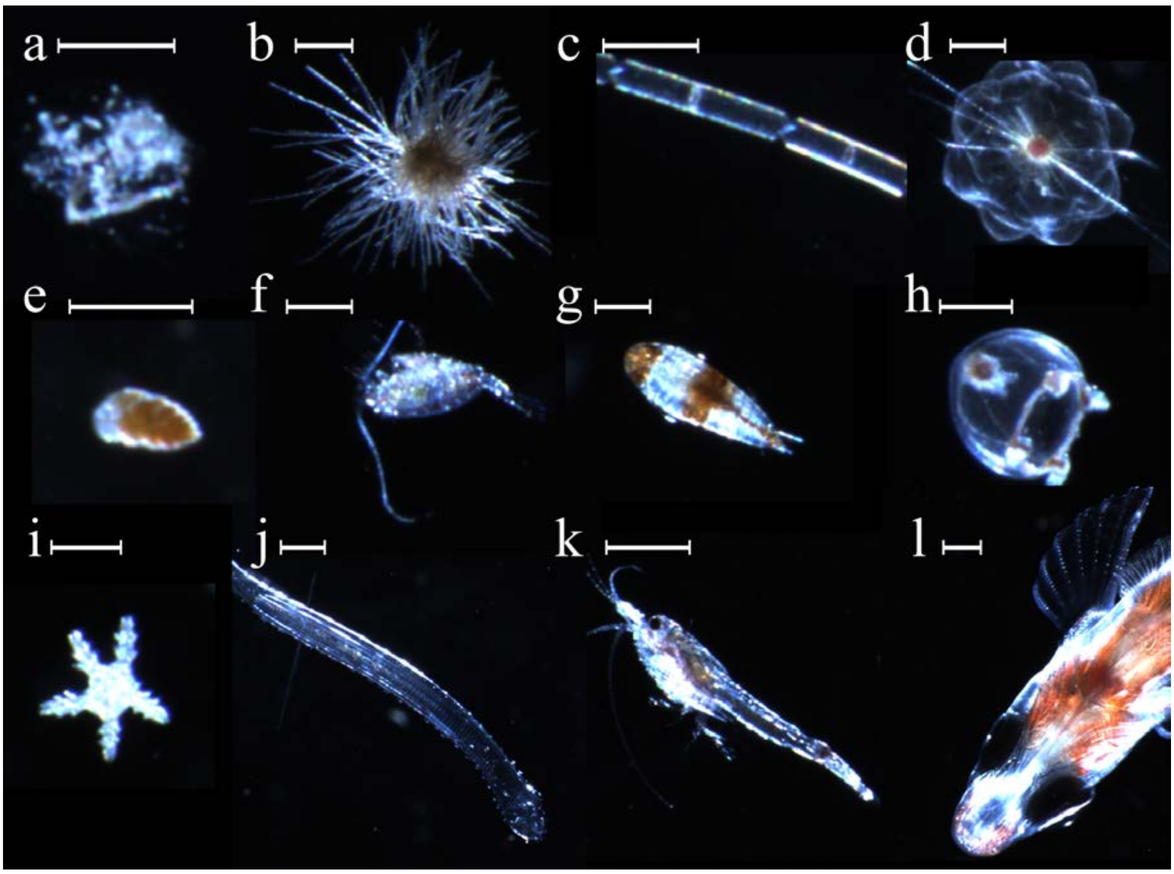

Figure 2. Examples of the 11 CPICS image categories: **a.** marine snow; **b.** *Trichodesmium* spp.; **c.** diatoms; **d.** radiolarians; **e.** foraminiferans; **f.** copepods; **g.** isopods; **h.** cnidarians; **i.-j.** 'other

zooplankton' (**i.** adult starfish; **j.** chaetognath); **k.** mysids; **l.** fish. Scale bar = 500 µm except for j, k, l: 1,000 µm.

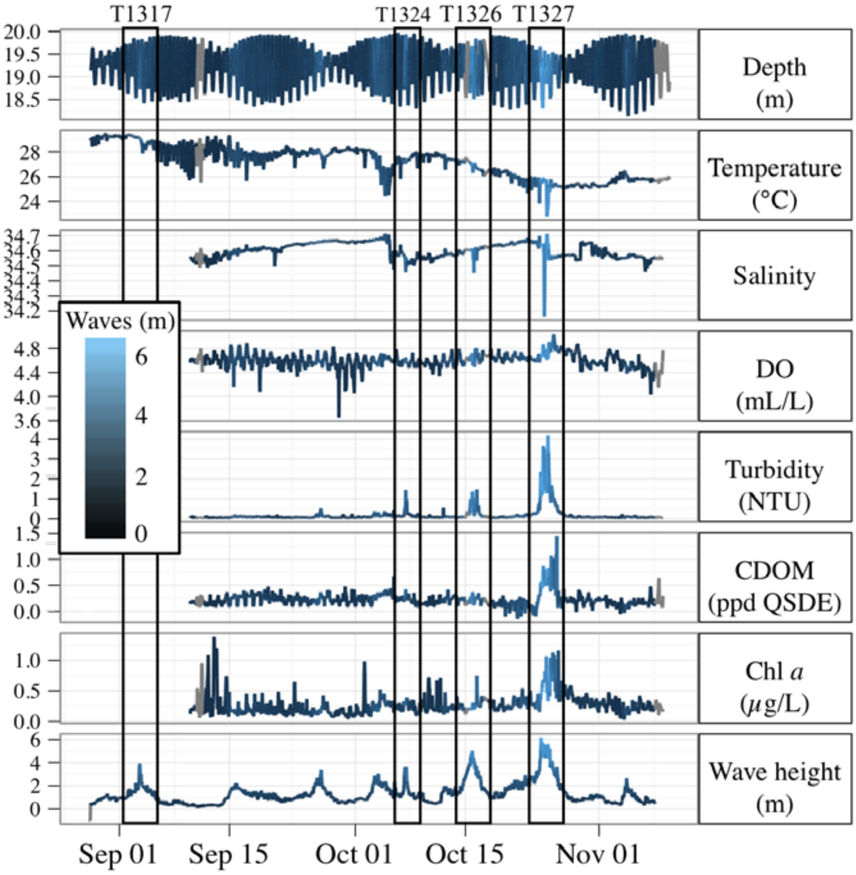

Figure 3. Temporal variation of depth (m), temperature (°C), salinity, dissolved oxygen (DO; mL/L), turbidity (NTU), CDOM (ppb QSDE), chlorophyll *a* (µg/L), and significant wave height (m) measured in the near-bottom layer at the observation site between August 28th and November 9th, 2013. Colour scale represents significant wave height (m). Boxes correspond to typhoons.

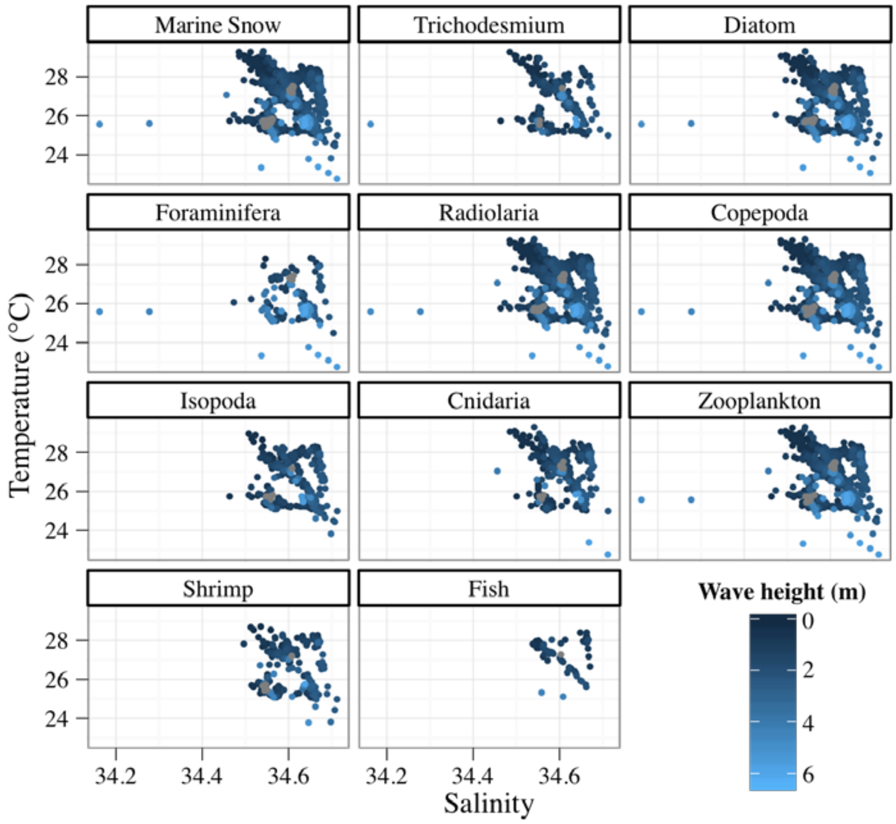

Figure 4. Distribution of marine snow and plankton categories depending on temperature and salinity during the sampling period. Colour scale represents significant wave height (m).

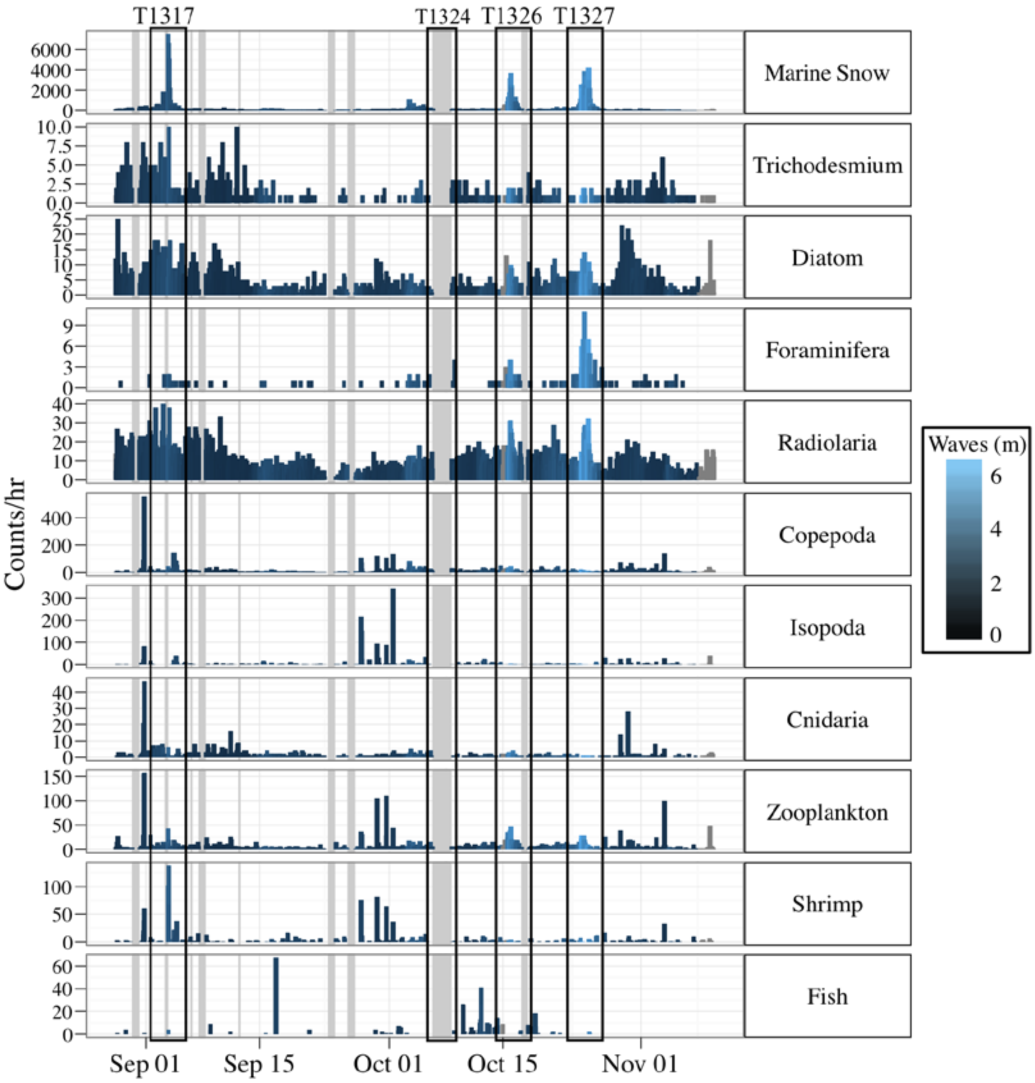

Figure 5. Temporal variation in abundance (counts/hr) of particle and plankton types during the sampling period. Gray shading indicates missing data. White boxes correspond to typhoons.

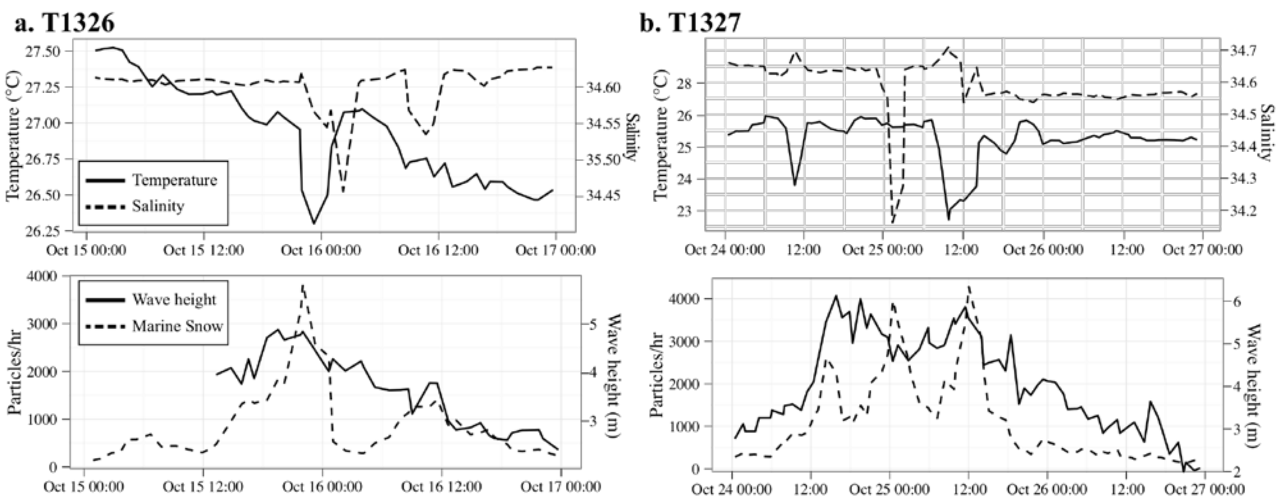

Figure 6. Salinity, water temperature (°C), significant wave height (m), and marine snow particle concentrations (particles/hr), during a. Typhoon T1326, b. Typhoon T1327.

Parameter	**Instrument**	**Measurement period**
Depth (m)	Acoustic Vector Current Meter (ADV), Nortek, USA	Aug.28 to Nov.09 ‘13
Temperature (°C)	ADV	Aug.28 to Nov.09 ‘13
Significant wave height (m)	Acoustic Doppler Current Profiler, RD Instruments, USA	Aug.28 to Nov.08 ‘13
Salinity	Water Quality Monitor (WQM), WETlabs, USA	Sept.10 to Nov.09 ‘13
Dissolved oxygen (DO) concentration (mL/L)	WQM	Sept.10 to Nov.09 ‘13
Turbidity (NTU)	WQM	Sept.10 to Nov.09 ‘13
Coloured dissolved organic material (cdom) (ppb QSDE)	WQM	Sept.10 to Nov.09 ‘13
Chlorophyll *a* (Chl *a*) concentration (µg/L)	WQM	Sept.10 to Nov.09 ‘13

Table 1. Characteristics and sampling period of measured physicochemical, environmental parameters.

	Median abundance (counts/hr)	Maximum abundance (counts/hr)	Relative nighttime abundance (%)	Total relative abundance (% of total plankton)	Temporal presence (%)
Trichodesmium	1	20	49.37	1.58	26
Diatom	3	36	48.58	9.28	76
Radiolaria	7	80	46.71	25.24	97
Foraminifera	1	10	45.51	0.43	8
Copepoda	8	574	65.84	36.27	97
Isopoda	2	334	97.24	5.11	23
Cnidaria	1	46	62.74	1.35	20
Other zooplankton	4	145	63.52	15.77	85
Mysidae	2	276	98.4	4.11	19
Fish	3	67	5.28	0.87	4
Marine Snow	79	14996	51.93		100

Table 2. Median and maximum abundance (counts/hr), relative nighttime abundance (100 * nighttime category abundance / total category abundance), total relative abundance (100 * total category abundance / total plankton abundance), and temporal presence (100 * number of hours present / total number of hours sampled) of particle and plankton types over the sampling period